Phys Chem Minerals (2006) 33: 403–416
DOI 10.1007/s00269-006-0086-x

ORIGINAL PAPER

Lars Olov Andersson

The positions of H^+, Li^+ and Na^+ impurities in beryl

Received: 21 November 2005 / Accepted: 4 April 2006 / Published online: 19 August 2006

Abstract Electron Paramagnetic Resonance (EPR) measurements show that Li^+ impurities are located at two different positions in beryl, one in the crystal lattice and the other in the crystal channel. The position of the Li^+ impurity in the lattice is generally assumed to be at the site of a missing Be^{2+} ion. It is shown that this is not the case, but that the Li^+ ion is located in a tetrahedron formed by the oxygens of one side of the Be tetrahedron and the nearest oxygen in the channel ring. This Li site has the coordinates (0.423, 0.344, 0.167) and can only be occupied when the neighbouring Be site is empty. There are four such sites around every Be tetrahedron at the distance of 1.46 Å from the Be site. The distance from the Li site to the oxygens of the Li tetrahedron is 1.84 Å. This compares favourably with the much smaller distance of 1.65 Å in the Be tetrahedron. Protons in beryl are trapped at or near these Li sites. Na^+ is known to be located at the 2b position at the center of the silicate rings, where it is stabilized by one water molecule located at each of the two surrounding 2a sites. This is also the position of Li^+ in the beryl channel. It is found that the presence of Na^+ in the ring of six oxygens reduces the radius of this ring. The Na^+ impurity has also been supposed to be located at position 2a alone and at 2b stabilized by only one water molecule. It is now proposed that Na^+ and H_2O are located together in the Al–Be plane when only one water molecule is associated with Na^+. The water oxygen is located at or near 2a and Na is closer to the Be site in tetrahedral beryl and closer to the Al site in octahedral beryl. It is proposed that the water protons are also located in the Al–Be plane, which would mean that there exists a third type of water in beryl. The origin of protons and OH^- ions in beryl is discussed and it is suggested that the plugs in the beryl channels are CO_3^{2-} ions. Diffusion of OH^- ions and natural radiation may have led to the creation of NO_3 and the blue colour of Maxixe beryl.

L. O. Andersson (✉)
Brunnenweid 49, 5643 Sins, Switzerland
E-mail: loandersson@bluewin.ch
Tel.: +41-41-7871048

Keywords Li in beryl · Beryl impurities · Maxixe-type beryl · EPR

Introduction

The ideal formula of beryl is $Be_3Al_2Si_6O_{18}$ and its space group is *P6/mcc*. The structure was first determined by Bragg and West (1926) and later refined by Gibbs et al. (1968) and Morosin (1972). The structure consists of six-membered silicate rings stacked upon each other so that their empty centers form channels in the *c*-axis direction. Neighbouring stacks are connected with beryl and aluminium ions in tetrahedral and octahedral positions, respectively. Six oxygens form a ring with an opening just large enough for a water molecule to pass. These oxygens are designated O(1) and the center of the ring is located at the position 2b in the *P6/mcc* unit cell. The other oxygens of the silicon tetrahedra are designated O(2) and they form the walls of cavities between the rings, large enough to accommodate CO_2 molecules and CO_3^{2-} ions. The center of the cavity is located at the crystallographic position 2a. The Be tetrahedra and the Al octahedra are formed by O(2) oxygens only.

In natural crystals, the beryl channels with their alternating rings and cavities contain many impurities, mainly H_2O and alkali ions. Other ions can substitute for Al^{3+}, Be^{2+} and Si^{4+} in lattice sites. The distribution and location of impurities in beryl has been the subject of many studies. Bakakin et al. (1969) suggested that the Li^+ impurity ion occupies the site of a missing Be^{2+} ion. The direct substitution of Li for Be has been accepted by practically all subsequent investigators, including Hawthorne and Cerny (1977), who also discussed the position of H_2O and Na^+ in the channels. They concluded that H_2O molecules must be located in the cavities, while Na and excess Li are located in the rings. They found that there is at least twice as much H_2O as Na in almost all beryls investigated and suggested that Na is stabilized at position 2b by a water molecule at one or, in most cases, both of the surrounding 2a positions. It has also

been suggested that Na is located at the 2a position, e.g. by Aurisicchio et al. (1988).

Wood and Nassau (1967) found from infrared absorption measurements that water molecules with two different orientations exist in the beryl channels. Type I water with the H–H vector parallel to the crystal *c*-axis direction is found in beryl with few impurities. In beryl with higher alkali contents, Type II water with the H–H vector perpendicular to the crystal *c*-axis direction is dominating. They also observed infrared absorption lines from CO_2 molecules in many beryl crystals.

Bakakin et al. (1970) studied the X-ray parameters and impurity contents of a large number of beryl crystals and found that they could be classified into octahedral beryls, where divalent cations are substituting for Al^{3+}, and tetrahedral beryls, where missing Be^{2+} ions are replaced by Li^{+}. Crystals with low impurity content show little lattice distortion and are classified as normal beryl. In octahedral beryl, the unit cell parameter *a* increases with the mean ionic radius of the ions substituting for Al, while the parameter *c* remains practically constant. In tetrahedral beryl, *c* increases with increasing number of Be vacancies, while *a* does not change much. Aurisicchio et al. (1988) obtained the same results from another large database and present a number of correlation diagrams, including one which shows that the number of Li impurities is practically equal to the number of missing Be atoms.

Sherriff et al. (1991) thoroughly discuss the effects of alkali impurities in beryl and give numerous references to earlier work in the field. Using NMR, they directly observed two different surroundings of Li in beryl and locate one Li in the channel and the other at the Be site. Manier-Glavinaz et al. (1989) have presented one study in which the results are not compatible with the location of the Li^{+} ion at the Be site. Andersson (1974) determined from EPR measurements that the Li^{+} ion is located at a distance of more than 1 Å from the Be site.

Sample details

The present work is based upon results obtained from Electron Paramagnetic Resonance (EPR) measurements (Andersson 1974, 1976, 1979) made 30 years ago in the laboratory of Varian AG in Zug, Switzerland. The EPR spectra were recorded at room temperature on Varian E-Line EPR spectrometers at 9.2 and 35 GHz. The single crystals of Maxixe-type beryl were mounted in the EPR cavity so that the magnetic field could be rotated in a plane containing the crystal *c*-axis. Since the EPR signals investigated here are axially symmetric, an additional rotation plane was not needed.

In 1972, a deep blue beryl was brought onto the gem stone market, but was later withdrawn because its colour faded after prolonged light exposure. The samples studied here are from this original material and the gem stone dealer who provided them reported that they contain Li, Mg, Mn, Na, K, Fe and Cs impurities. Nassau et al. (1976) were able to produce a similar colour in certain beryls by gamma ray, X-ray and neutron irradiation and studied the infrared absorption spectra of these crystals. They were called Maxixe-type beryls, because the colour and its fading were reminiscent of the Maxixe beryl found in 1917 (Wild 1933). The Maxixe beryl was blue when it was taken out of the mine, but the colour of Maxixe-type beryl was artificially created. Bastos (1975) states that the untreated material is a light pink morganite from Barra de Salinas in Minas Gerais, Brazil. He states that the material was not irradiated by X-rays, gamma rays, neutrons, protons or electrons, but treated with a "secret method" by the Halba company, which sold them under the trade name Halbanita Aquamarine.

One of the samples for this study was heated until the blue colour disappeared and it was then light pink. It also showed the Mn lines in the EPR spectrum typical of morganite beryl. With the help of UV irradiation it was possible to recreate the blue colour.

It should be noted that EPR measurements give results for the surrounding of one specific lattice defect, which may occur in only few of the unit cells, while results from X-ray or neutron diffraction measurements represent an average of all lattice defects in the crystal. The absence of one Be and the presence of one Li near one of the defects studied by EPR indicate that the sample studied is a tetrahedral beryl. The unit cell dimensions, which can confirm this classification and depend on the average concentration of impurities in the crystal, can be determined by X-ray measurements. Unfortunately, there are no unit cell dimensions available for the Maxixe-type beryl. This does not influence the interpretation of the EPR results, but some of the calculated distances need to be corrected when the exact dimensions are known. These corrections are on the order of 1%, which represents the possible variation of the unit cell dimensions.

Li^{+} in the lattice site

It is generally assumed that the Li^{+} impurity is substituting for Be in beryl, in spite of the large differences in ionic diameters. It will be shown here that there exists another site in the beryl lattice with more space for the Li^{+} ion. The distance from the crystallographic site 2a to the Li nucleus can be calculated from a special EPR experiment and it agrees with the distance to this other Li site. The assumed location at the Be site is not compatible with the EPR results. The implication of this to the interpretation of earlier investigations of beryl will be discussed. It is very likely that H^{+} impurities in beryl are also located at the described lattice site.

Geometric calculations

The following calculations are based on positional parameters[1] determined by Brown and Mills (1986) for a beryl crystal with unit cell dimensions $a = 9.236$ Å and $c = 9.246$ Å. This is a tetrahedral beryl containing considerable amounts of water and alkali ions and it is expected that the Maxixe-type beryl has similar unit cell dimensions. In order to estimate possible variations in the results, calculations are also made using parameters determined by Morosin (1972) for a synthetic crystal containing very few impurities and with unit cell dimensions $a = 9.2088$ Å and $c = 9.1896$ Å. The results (those for the synthetic crystal are shown in brackets) are given with an accuracy of three decimals to allow better comparisons, even if the last decimal may not be significant.

To simplify their identification, some of the rings and cavities in the unit cell have been labelled with letters. Cavity A is centered at (0, 0, ¼) between Ring K centered at (0, 0, 0) and Ring L at (0, 0, ½) in one channel. In the neighbouring channel, Cavity B is centered at (1, 0, ¼) between Ring M at (1, 0, 0) and Ring N at (1, 0, ½). Cavity C is centered at (1, 0, ¾) between Ring N and Ring O at (1, 0, 1). Cavity D is at (1, 0, −¼) between Ring M and Ring P at (1, 0, −½). Cavity E is centered at (1, 0, −¾). This labelling is illustrated in Fig. 1 and will often be referred to in the following discussions.

If the Be^{2+} ion is missing from the Be tetrahedron between Cavity A and Cavity B in tetrahedral beryl, it has been assumed that the Li^+ ion is substituting for it at the Be site (½, 0, ¼). At that site, the distance to the nearest oxygens is 1.653 Å in the normal beryl and has increased to 1.675 Å in the tetrahedral beryl. It could be expected that the distance should have increased much more because of the large difference in ionic diameters of Li and Be. A more likely position for the Li^+ ion will now be calculated.

Two of the Be tetrahedron surfaces face Cavity A, one directed towards Ring L and the other towards Ring K. The three oxygens of the latter surface form another distorted tetrahedron together with the oxygen atom in Ring K which is closest to the Be tetrahedron. The edges of this new tetrahedron have been indicated in Fig. 1. I propose that the Li^+ ion is located in this tetrahedron. The position of the Li^+ ion is obtained by placing it at equal distance from all four oxygens of the tetrahedron. Through iteration to three decimals, this distance is found to be 1.864 Å (1.843 Å), which gives the Li^+ ion much more space than in the Be tetrahedron. The coordinates for this site are (0.423, 0.343, 0.167) in the tetrahedral beryl and (0.423, 0.344, 0.167) in the normal beryl. This position will henceforth be referred to as the Li site.

Three of the oxygens in the Li tetrahedron belong to Cavity A and one to Cavity B. The Li site is very close to the surface formed by the Cavity A oxygens, only 0.231 Å (0.212 Å) away. When the Li^+ ion exits through this surface, it enters Cavity A. The three other surfaces of the Li tetrahedron are blocked for passage by silicon atoms at 2.269 and 2.476 Å from the Li site and by another oxygen at 2.256 Å. This is the fifth oxygen mentioned by Andersson (1974). The described site forms an easily accessible trap for a Li^+ ion in Cavity A.

Equivalent Li sites are found in the tetrahedra formed by the other three sides of the Be tetrahedron and the nearest oxygens in Rings L, M and N. There are therefore four Li sites close to each Be tetrahedron. Their distance to the Be site is 1.470 Å (1.457 Å). There are 12 Li sites in each cavity, 6 of them closer to one ring and 6 closer to the other.

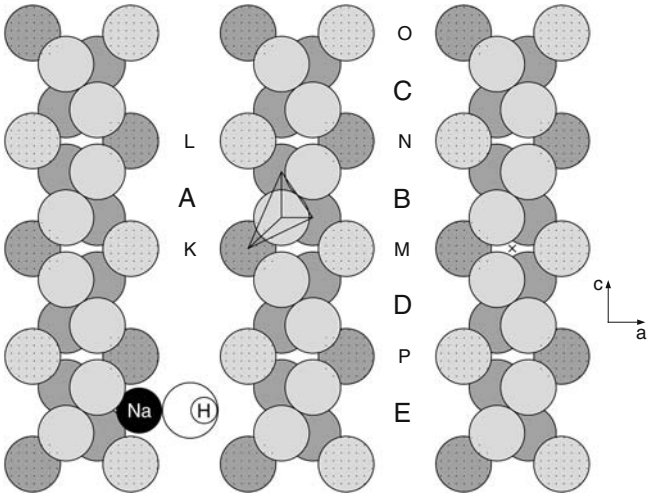

Fig. 1 Schematic representation of two neighbouring channels in the beryl crystal structure. Channel cavities are labelled with *large capitals* and channel rings with *small capitals* for reference. The oxygen atoms are shown as *shaded circles*, those below the c-a plane darker than those above the plane. O(1) oxygens are shaded with a *dotted screen*. The smaller Si, Be and Al atoms are not shown. The proposed location of a Na^+ ion next to a water molecule is illustrated in the *left channel*. The Li tetrahedron is indicated at the *center*

Experimental results

The location of an Li^+ ion at the Li site described above is experimentally supported by the results of EPR measurements in Maxixe-type beryl (Andersson 1974). Some of the electrons which are released by the irradiation which creates the Maxixe-type beryl are trapped by H^+ impurities to form H° atoms. These atoms are located at the center of empty channel cavities and give a strong doublet signal in the EPR spectrum. A number of spin-flip satellite lines caused by the simultaneous flip of the electron spin and the spins of nearby nuclei were observed close to each of the two lines. The satellite lines around one hydrogen line are shown in Fig. 2.

The distance from the unpaired electron of the hydrogen atom to the surrounding nuclei can be

[1]The value of x for O(2) at 24°C in Table 4 is certainly a printing error and 0.4985 is used instead.

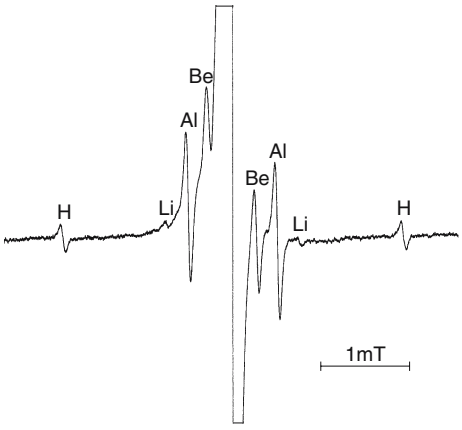

Fig. 2 Satellite lines around the high-field hydrogen line in the room temperature 35 GHz EPR spectrum of Maxixe-type beryl, with the magnetic field direction making an angle of 52° with the crystal *c*-axis. The main line has been truncated in the figure

calculated with great accuracy from the intensity of the satellite lines. The observed intensities of the Al and Be satellite lines will first be compared with the intensities calculated from the known distances to these nuclei. Then the intensities of the Li and H satellite lines will be compared with intensities calculated from different assumptions about the location of these nuclei.

The theory for the satellite lines has been developed by Trammel et al. (1958). The spacing of each satellite is proportional to the magnetic moment of the nucleus, which makes it easy to identify the nucleus involved. The relative intensity of the satellites is given by a complicated formula, where many terms can be neglected for EPR measurements in high magnetic fields. Trammel et al. (1958) have calculated a simpler expression for neighbouring protons in their equation (24). The satellite intensity is strongly dependent on the distance from the unpaired electron to the surrounding nuclei. When the distance r is the same to all neighbour nuclei of the same kind, the formula can be further simplified to

$$R = 9r^{-6}H^{-2}(g_e\beta_e)^2S/8$$

Here R is the ratio of the intensity of one satellite line to that of the main line, H is the magnetic field used in the experiment, g_e is the g-factor and β_e the magnetic moment of the unpaired electron and S is a sum over all surrounding nuclei. Each term in this sum is defined as $\sin^2\theta\ \cos^2\theta$, where θ is the angle between the magnetic field direction and the vector from the unpaired electron to the nucleus. The above formula is valid for nuclei with a spin of ½. For Be and Li with spin 3/2 the factor 9 will be replaced by 45 and for Al nuclei with spin 5/2 it will be replaced by 105.

The intensities measured by Andersson (1974) refer to pairs of satellites and have to be halved to give $R_{Be} = 0.135\%$, $R_{Al} = 0.17\%$ and $R_{Li} = 0.006\%$ in a field of 1.275 tesla and $R_H = 0.245\%$ in a field of 0.350 tesla. These experimental results will now be compared with calculations of R using atomic distances. All the following calculations are based on the room temperature lattice parameters determined by Brown and Mills (1986).

In a first approximation, we consider only the nearest six Al and six Be neighbours, which are all in the same plane as the H° atom. When the magnetic field direction is in this plane, which is perpendicular to the *c*-axis, $S = 0.75$ for the six Al and also for the six Be. The results are equal for Al and Be because their symmetry around H° is identical. When the magnetic field is directed along the *c*-axis, $S = 0$ and when it forms an angle $\phi = 45°$ with the *c*-axis, $S = 15/16$. The maximum value $S = 1$ for the six nuclei is obtained for $\phi = 54.74°$.

The ratio of the intensities of Be and Al satellites is

$$\frac{R_{Be}}{R_{Al}} = \frac{45}{105}\frac{r_{Al}^6}{r_{Be}^6}\frac{S_{Be}}{S_{Al}}$$

For the nearest neighbours $S_{Be}/S_{Al} = 1$ and $r_{Al}/r_{Be} = 2/\sqrt{3}$. Therefore, $R_{Be}/R_{Al} = 64/63$. Since the measured ratio is considerably lower than 1, Andersson (1974) concluded that only 5 Be atoms are contributing to the S_{Be} sum.

S should be zero when the magnetic field direction is parallel to the *c*-axis, but the observed intensity of the satellite lines at this angle is considerable. We therefore have to consider the contribution from other Be and Al neighbours. For the twelve next-nearest neighbours the symmetry is different for Be and Al, so S_{2Be} will be different from S_{2Al} . For $\phi = 0°$, S_{2Be} is 3.000 and S_{2Al} is 2.939 and for $\phi = 54.74°$, S_{2Be} is 1.167 and S_{2Al} 1.143. Since the distance from H° to these next-nearest neighbours is larger than to the nearest ones, these sums have to be divided by the sixth power of the ratio of these distances before they are added as corrections to the sums of the six nearest neighbours.

By including also the third and fourth nearest neighbours in the calculation, one obtains the corrected values $S_{Be} = 0.389$ and $S_{Al} = 0.582$ for $\phi = 0°$, $S_{Be} = 1.161$ and $S_{Al} = 1.254$ for $\phi = 54.74°$ and $S_{Be} = 0.993$ and $S_{Al} = 1.145$ for $\phi = 90°$, to be compared with the values $S = 0$, $S = 1$ and $S = 0.75$ for the nearest neighbours. The angular variations in the relative intensities of the lines, due to the different S values, are observed in the experimental spectra. However, the absolute amplitudes of the lines show much larger angular variations. These are due to the dipole broadening of the EPR signal from the surrounding nuclei. Since the integrated intensity of the signal is constant, its amplitude decreases when the line is broadened. If this broadening is due mainly to a proton located in the *c*-axis direction, the minimum broadening and the largest amplitude will be found at $\phi = 54.74°$. The maximum is observed at about $\phi = 52°$. Since the relative intensities at this angle deviate negligibly from those at 54.74°, the experimental evaluations were made at maximum amplitude. The following calculations will

be made for $\phi = 54.74°$. The results for the different nuclei are summarized in Table 1.

When one of the nearest neighbour Be is missing, the corrected value for S_{Be} is 0.994 instead of 1.161. The intensities of the Be and Al satellites in percent of the intensity of the main line in a magnetic field of 1.275 tesla are then $R_{Be} = 0.122\%$ and $R_{Al} = 0.152\%$, which gives $R_{Be}/R_{Al} = 0.805$. If there are six nearest Be atoms, $R_{Be}/R_{Al} = 0.94$. The ratio measured by Andersson (1974) is 0.27/0.34 or 0.79, which is in good agreement with the calculated value for only five Be atoms next to the hydrogen atom.

The Be and Al satellites are well resolved only around $\phi = 54°$, where the dipolar broadening is smallest and in the high magnetic field, where the splitting is largest. However, the relative intensity of the satellite line is smaller in the higher field, as can be seen from the formula for R. The signal-to-noise ratio can be increased by using a higher microwave power, but it has to be avoided that the signals get saturated. The line width of the Be and Al satellites is found to be the same, so the signal-to-noise ratio is the only error source in the comparison of the unsaturated lines. When this error source is considered, the value of the measured ratio R_{Be}/R_{Al} is limited to the range 0.73 to 0.85.

When the intensity of the satellite line is compared directly with that of the main line, one also has to consider the error sources in the determination of R which arise from the smaller line width and easier saturation of the main line. The signal intensities therefore have to be obtained by integration and the amplitudes have to be corrected using saturation curves. The value R_{Al} measured as 0.17% could vary from 0.14 to 0.20% due to the uncertainties of these calibrations. The calculated value 0.152% for R_{Al} is within this range and will be used as reference for the measurements of the intensities of the Li and H satellite lines. The comparison of these intensities with that of the Al satellite line eliminates the additional error sources and gives a more accurate result than the direct comparison with the main line. The error limits of the measured ratios are stated in Table 1 and it is indicated if the results were obtained by a direct measurement or in comparison with the Al reference.

The measured intensity of the Li satellite is 4% of that for the Al satellite and therefore $R_{Li} = 0.006\%$. There are six cavities surrounding the hydrogen atom in the Al–Be plane and in each of these there are two equivalent Li sites nearest to the Be sites between these cavities and the cavity containing H°. The sum S for all

Table 1 Calculated values of the satellite intensity R for different nuclei at different distances from the unpaired electron of a hydrogen atom located at (1, 0, ¼)

Nucleus	Number of neighbours	Distance in Å	Field in Tesla	Calculated R in %	Comment	Nucleus	Field in Tesla	Measured R in %	Method
Al	6	5.332	1.275	0.121		Al	1.275	0,17 +/– 0,03	direct
Al	all	various	1.275	0.152		Al	1.275	0,152 +/– 0,000	reference
Be	6	4.618	1.275	0.123					
Be	5	4.618	1.275	0.102		Be	1.275	0,135 +/– 0,030	direct
Be	all	various	1.275	0.143		Be	1.275	0,121 +/– 0,010	reference
Be	one missing	various	1.275	0.122					
Li	1	4.618	1.275	0.0189	Be site				
Li	1	5.785	1.275	0.0047	Li site	Li	1.275	0,006 +/– 0,002	reference
Li	1	5.164	1.275	0.0068	site (½,0,0)				
Na	1	6.935	1.275	0.0024	site (1,0,1)				
H	2	4.107	0.350	0.274	oxygen	H	0.350	0,245 +/– 0,070	direct
H	2	4.107	1.275	0.0206	at 2a	H	1.275	0,018 +/– 0,003	reference
H	2	4.171	0.350	0.250	center of				
H	2	4.171	1.275	0.0189	gravity at 2a				
H	1 + 1	3.910+5.412	1.275	0.0162	Type I				
H	2 + 2	3.910+5.412	1.275	0.0325	Type I				
H	4	4.721	1.275	0.0176	Type III				

The measured values, obtained by direct comparison with the main line or with the Al satellite intensity as reference, are listed to the right

these sites is 1.931. Since only one of these Li sites is occupied, the sum has to be divided by 12, and since the abundance of ^{7}Li is only 92.58%, the result has to be multiplied with that percentage. We then obtain $S_{Li} = 0.149$. If the Li^+ ion were located at the Be site, $S_{Li} = 0.154$. The distances are $r = 5.785$ Å for the Li site and $r = 4.618$ Å for the Be site. In the field of 1.275 tesla, we then obtain $R_{Li} = 0.0047\%$ for the Li site and $R_{Li} = 0.0189\%$ for the Be site. If the Li^+ ion were located at the Be site, the Li satellite intensity should be about equal to that observed for the H satellite in Fig. 2. From the measured result, the distance from H° to the Li nucleus is determined to be 5.6 ± 0.3 Å. The distance of 5.785 Å to the Li site is within this range, which supports the assumption that the Li^+ ion is located at the Li site. If the unit cell dimensions of the Maxixe-type beryl were known, the calculated distance may be different, but not by more than 1% from 5.785 Å.

There exists another interstitial site in the beryl lattice, large enough for a Li^+ ion, at position (½, 0, 0). One such site is marked with a cross to the right in Fig. 1. This site is surrounded by four O(2) oxygens at 1.90 Å, two O(1) oxygens at 2.17 Å and two Si at 1.82 Å. With $S = 0.107$ for $\phi = 54.74°$ and $r = 5.164$ Å, one obtains $R = 0.0068\%$ for the satellite line from a Li nucleus located at this site. This value is within the measurement limits, so the EPR result cannot eliminate the possibility that the Li ion is located at (½, 0, 0). However, the distance to the positive Si ions is short and a Li ion cannot access this site from the beryl channel.

The comparison of the measured intensities with those calculated confirms that a Li^+ ion occupies a Li site in Cavity A next to the empty Be site between Cavity A and Cavity B when Cavity B is occupied by a H° atom. Andersson (1974) found that there are approximately 2×10^{17} hydrogen atoms per cm^3 in the Maxixe-type beryl. This means that, although there is one Li^+ ion in a Li site for every missing Be, the configuration with the H° atom exists in only 1 out of 20,000 cavities.

Discussion

The Li^+ ion compensates for only one of the charges of the missing Be^{2+} ion and a second ion is needed for complete charge compensation. The following study of the second ion supports the location of Li^+ and H^+ impurities at the Li site and explains some observations made in beryl crystals.

When the four Li sites next to the empty Be site between Cavity A and Cavity B in Fig. 1 are considered, there are several possibilities for the compensation of the charges of the missing Be^{2+} ion:

(1) Li^+ at a Li site in Cavity A and Cs^+ at the center of Cavity B
(2) Li^+ at a Li site in Cavity A and Na^+ in Cavity B
(3) Li^+ at a Li site in Cavity A and Li^+ at a Li site in Cavity B
(4) Li^+ at a Li site in Cavity A and H^+ at a Li site in Cavity B
(5) H^+ at a Li site in Cavity A and H^+ at a Li site in Cavity B
(6) Li^+ at a Li site in Cavity A and Na^+ in Ring N

It is unlikely that a second cation exists in the same cavity as the Li^+ ion.

Case (1) is regularly observed in beryls which contain Cs. The difference to earlier models is that the Li^+ ion is located at a Li site and not at a Be site. The number of Li impurities is usually larger than that of Cs, so Cs is always accompanied by Li. The size of the Cs^+ ion is so large that it fits well into the cavity when it is located at position 2a. The smaller Rb^+ and K^+ ions cannot be so well stabilized in this position and are less common impurities in beryl.

The Na^+ ion in Case (2) is even smaller and less likely to be stabilized at the 2a position, even if some authors have located it there. Na is a common impurity in beryl and it will later be suggested how it can be stabilized in the cavity by a water molecule.

Case (3) was proposed by Sherriff et al. (1991) using fictive Li positions near the cavity walls. However, this proposal was immediately rejected because there would be no need for additional Na^+ and Cs^+ ions in the channels when the two Li^+ ions compensate for the missing Be^{2+} charge. A further argument is that there is not enough Li in most beryls to supply two ions for every missing Be. Even if it is not common, the configuration in Case (3) may still exist, because the Li sites in the different cavities are more than 2.5 Å from each other. It is less likely that the two Li sites in the same cavity, at a distance of 1.99 Å from each other, are simultaneously occupied.

Case (4) is the precursor of the configuration studied in the EPR measurements. The H^+ ion is located at a Li site and when it captures an electron released during the irradiation which creates the Maxixe-type beryl, it forms the hydrogen atom observed by EPR. The fact that the hydrogen EPR signal disappears upon heating and is recreated by renewed irradiation, supports the assumption that the proton moves back and forth from the Li site to the 2a site in the same cavity during these events. If this were a common case, we would have the same problem as in Case (3), that there is no need for additional Na^+ and Cs^+ ions in the channels.

Case (5) is less likely to occur in nature, but will be used to give an explanation of the observations made by Manier-Glavinaz et al. (1989). They leached the cations out of the channels in beryl by adding HCl to the crystals at high temperature. At last all cations had been replaced by H^+. The surprising result was that there was no large difference in the leaching of Cs, Na and Li. They therefore could not support the assumption that Li is located at the less accessible Be site. As we have seen in Case (4), there is no need for additional Na^+ and Cs^+ ions in the channels when a Li site in Cavity B is occupied by H^+. The cations are therefore leached out when the

added H^+ ions are trapped at Li sites in the experiment of Manier-Glavinaz et al. (1989). An added H^+ ion can also be momentarily trapped at the Li site next to the site occupied by a Li^+ ion in Cavity A. If the Li site is a stronger trap for protons than for Li, the H^+ ion will remain in its trap and the neighbouring Li^+ ion will be leached out, as observed by Manier-Glavinaz et al. (1989). The proton may not be located exactly at the same position in the Li tetrahedron as a Li^+ ion, but has probably formed an OH bond with one of the oxygens. It could also form a hydrogen bond, most likely between the O(1) oxygen and the O(2) oxygen which is at a distance of 2.61 Å from the O(1) oxygen. Manier-Glavinaz et al. (1989) observed a line at 3699 cm^{-1} in the infrared spectrum, for which the intensity increases with the amount of introduced H^+ ions and which can be associated with the OH bond.

Case (6) occurs when the number of water molecules is so large that there is water in both Cavity B and in Cavity C. The Na^+ ion from Case (2) then finds a more stable position in Ring N between two Type II water molecules. This configuration gives a medium-range rather than a short-range charge compensation.

Cases (1), (2) and (6) are common in beryl crystals. Case (1) with Rb^+ and K^+ occurs less often, while the other cases described are very rare in nature. When there are two empty Be sites next to each other, a divalent cation like Ca^{2+} can replace two Na^+ ions and will be located in the ring like Na in Case (6).

Li^+ in the channel

Many studies, like that of Sherriff et al. (1991), have shown that Li^+ ions exist also in the beryl channels, but the exact location has not been determined. The results of EPR measurements now indicate that the Li^+ ions are located at the center of the oxygen rings at the crystallographic position 2b.

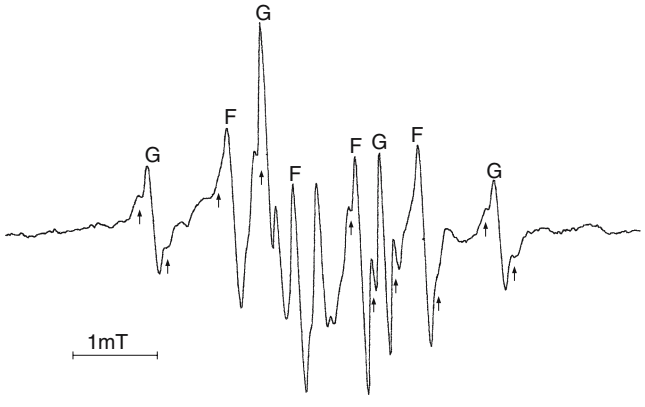

Fig. 3 The room temperature EPR spectrum of Maxixe-type beryl at 9.2 GHz with the magnetic field parallel to the crystal *c*-axis. The lines of the two quartet signals have been labelled with *F* and *G*. *Arrows* show some of the water proton splittings

Experimental results

A large number of EPR signals are observed in the irradiated Maxixe-type beryl. The signals marked F and G in Fig. 3 can be clearly separated by a special out-of-phase detection technique, as demonstrated by Andersson (1976). These signals have been identified from their *g*-values to arise from CO_2^- (Andersson, to be published). The axial symmetry of the EPR *g*-values indicates that the CO_2^- radical is rotating rapidly around its symmetry axis, which is oriented along the crystal *c*-axis.

Each of the signals F and G consists of four lines, arising from hyperfine splitting by nuclei with spin $I = 3/2$ interacting with the CO_2^- radical. ^7Li, ^{23}Na and ^{39}K have spin 3/2, are common impurities in beryl, and can as positive ions be associated with the CO_2^- radical. Another signal with similar *g*-values is also observed. This signal shows no splitting and is therefore associated with a cation without nuclear spin, probably Ca^{2+}.

When the cations are located on the *c*-axis, they stabilize the CO_2^- radical in the described orientation. Because of the bent structure of the CO_2^- radical, its oxygens are farther from the cavity walls than the oxygens of the linear CO_2 molecule, which facilitates the free rotation. The ring oxygens prevent much movement in the *c*-axis direction, so the CO_2^- radical must be located near the center of the cavity. The only space left for the cation is then in one of the rings surrounding the cavity with the CO_2^- radical. Since K^+ is too large to fit into the ring, this ion can be eliminated as a source of the splitting.

The ratio of the isotropic splittings of the EPR quartets is similar to the ratio of the isotropic hyperfine couplings of Li and Na. The slight difference can be the result of a somewhat different electron density at the two nuclei. The splitting of signal F corresponds to an unpaired electron density of 4.5% at the Li nucleus and the splitting of signal G corresponds to a density of 3.9% at the Na nucleus. This may indicate that the Li^+ ion is slightly closer to the CO_2^- radical, which is possible because of its smaller size. This could be a more stable position for the small Li^+ ion than exactly at the center of the ring.

When the EPR spectrum is simulated from its components, it is found that all lines of signals F and G are further split into three lines with the approximate ratio of 1:4:1 with a very small splitting. Some of the outer lines are resolved in the total spectrum and are indicated with arrows in Fig. 3. A ratio of 1:2:1 would be expected if some electron density is delocalized on a type II water molecule which is stabilizing the cation in the ring together with the CO_2^- radical. The higher intensity observed for the central line could be an artifact of the simulation, but could also indicate that some of the cation signals are not split by a neighbouring water molecule and therefore only contribute to the central line.

The intensity of signal F is roughly equal to that of signal G, but much smaller than the intensity of the H°

signal, so the observed configuration is very rare. Signals F and G disappear upon heating of the crystal to 150°C, while the signal from H° disappears only around 180°C. This is in agreement with the observation by Nassau et al. (1976) that the release of electrons occurs in more than one step.

Discussion

The important result of the EPR experiment is that the Li^+ ion is observed in the same surrounding as the Na^+ ion. Both are located at 2b in the channel, at the center of the oxygen ring. No EPR signal can be observed from the large majority of the cations, which are located between two water molecules. A small fraction of the cations are located in a ring between one cavity containing H_2O and another cavity containing CO_2. This configuration can be detected by EPR only when the CO_2 molecule captures an electron to form a CO_2^- radical. The majority of the Li^+ ions at position 2b in the ring are stabilized by two water molecules like Na^+ in Case (6). This is the only location for Li^+ in the channel, because a Li^+ ion in the cavity will soon be trapped at a Li site.

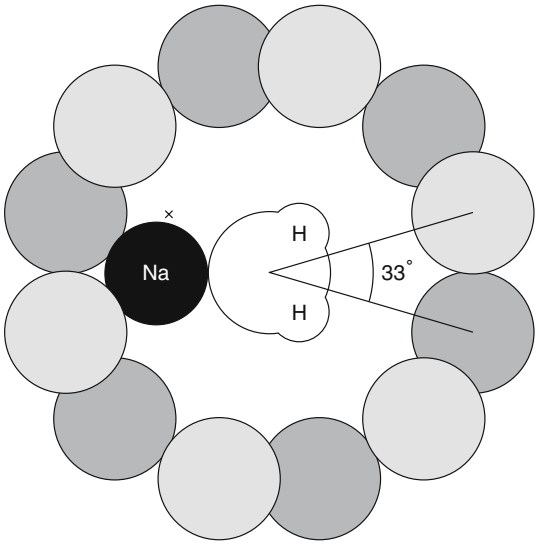

Fig. 4 The projection on a plane normal to the crystal *c*-axis of two layers of O(2) oxygen atoms belonging to different silicate rings. A water molecule is located with its oxygen atom at position 2a on the crystal *c*-axis in a plane halfway between the oxygen planes. The Na^+ ion is shown between the cavity wall formed by the O(2) oxygens and the water molecule in the position next to a missing Be^{2+} ion. The *cross* indicates its position next to a replaced Al^{3+} ion

Na^+ and H_2O in the channel

In some of the references mentioned in the Introduction, Na is located at 2a and H_2O at 2b, while in others Na is located at 2b and H_2O at 2a. The most likely situation is that H_2O is located at 2a and that Na can be located both in the cavity and in the ring. When there are no impurities in the neighbourhood of a water molecule, it is oriented as Type I water in the cavity. When there is a Na^+ impurity close to a single water molecule, I suggest that they are both located in the same cavity, with a new type of orientation of the water molecule. The possibility of such a configuration will be investigated by geometric calculations and it will be discussed how the existence of this configuration influences the interpretation of infrared absorption spectra. When there are two water molecules next to a Na^+ impurity, the Na^+ ion is located in the ring and the surrounding water molecules are oriented as Type II water. The location of Na at 2b is in agreement with the above EPR results. The position of the Type II water molecule can be determined by EPR measurements.

Na^+ in the cavity: geometric calculations

As mentioned in the discussion of Case (2), the Na^+ ion is not likely to be in equilibrium at 2a. The Na^+ ion is too large to enter the Li tetrahedron, but it can pass between the oxygens of the two rings if it is moved in the *a* axis direction from the center of the cavity. However, before it has come so far, it will be stopped by the oxygens of the Be tetrahedron. This position between two ring oxygens and two Be tetrahedron oxygens could be considered as a loose trap for the Na^+ ion. If a water molecule is located with its oxygen at the cavity center, the trap is very effective. This configuration is illustrated in the bottom left cavity of Fig. 1 and in the plane perpendicular to the *c*-axis in Fig. 4.

When the Na^+ ion is at equal distance from the two O(2) oxygens of the Be tetrahedron and the water oxygen at 2a, this distance is 2.251 Å in the normal beryl. The distance to the O(1) oxygens is 2.386 Å. Since the corresponding Na–O distances in tetrahedral and octahedral beryl are less than 0.01 Å larger than in the normal beryl, only the distances obtained from the parameters of Morosin (1972) are reported here. A similar trap exists in the direction to the Al^{3+} ion, but here the two limiting oxygens belong to different Be tetrahedra. The location of the Na^+ ion in this case is indicated with a cross in Fig. 4. When the Na^+ ion is at equal distance from the two O(2) oxygens closest to the Al^{3+} ion and the water oxygen, its distance from the cavity center is 2.221 Å. The distance to the O(1) oxygens is here 2.430 Å. The distances from Na to the O(2) oxygens are rather short in both cases, but would increase if the Na^+ ion were located closer to the oxygen of the water molecule or if the water oxygen were shifted slightly off-center.

The calculated Na–O distances can be compared with the distance from the Na^+ ion at 2b to the oxygens of the surrounding Type II water molecules in different beryls. It is 2.312 Å in the tetrahedral beryl and 2.298 Å in the octahedral beryl if the water oxygens are located

at 2a. If the center of gravity of the Type II water molecules is located at 2a, the Na–O distance is 2.247 Å in the tetrahedral beryl and 2.233 Å in the octahedral beryl. The room temperature parameters of Brown and Mills (1986) are used to calculate distances in tetrahedral beryl, and for octahedral beryl the X-ray parameters of Artioli et al. (1995) are used.

Na^+ in the cavity: discussion

Schmetzer (1989) investigated the infrared spectra of many different beryl crystals and found that the intensities of the three dominant absorption bands in the OH stretching region vary independently from each other. He therefore concluded that three different types of water exist in beryl. He relates band A at 3694 cm^{-1} to Type I water, which is located in a cavity without any cations, and band B at 3592 cm^{-1} to the pair of Type II water molecules which trap the Na^+ ion in the ring. The band C at 3655 cm^{-1} was assumed by Wood and Nassau (1967) to arise from the same Type II water molecules as band B, but Schmetzer (1989) relates it to a Type II water molecule which stabilizes Na^+ at 2b without the help of a second H_2O. But why should the vibration mode of the Type II water molecule be different when there is no water molecule in the neighbouring cavity? Instead, I suggest that the third type of water is the molecule stabilizing the Na^+ ion in the Al–Be plane as shown in Fig. 4. If the protons of this water molecule are located in the same plane, there will be no infrared absorption by this water molecule when the electric field is directed parallel to the crystal *c*-axis, which is when bands A and B are observed. There will only be an absorption with the field in the perpendicular direction, where band C is observed.

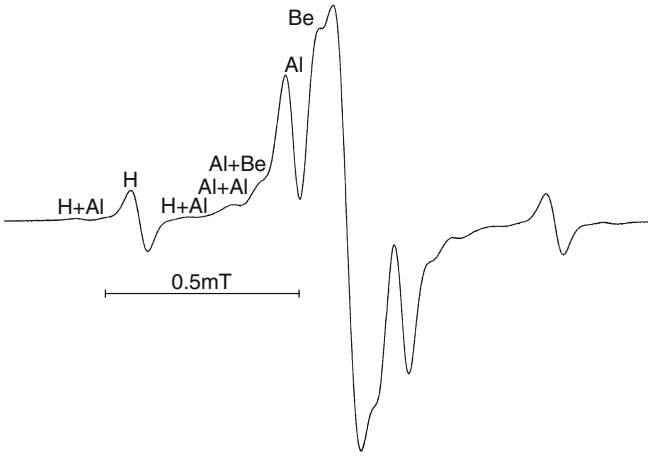

Fig. 5 Satellite lines around the high-field hydrogen line in the room temperature 9.2 GHz EPR spectrum of Maxixe-type beryl, with the magnetic field direction making an angle of 52° with the crystal *c*-axis. This spectrum is obtained at such high microwave power that the main line is almost completely saturated

Iron is a common impurity in beryl. As Fe^{3+} it can substitute for Al^{3+} at the lattice site and in the channel it can be found as Fe^{2+}. The Fe^{2+} ion is smaller than the Na^+ ion, so it could be stabilized in the cavity by a water molecule as illustrated for Na^+ in Fig. 4. Colour changes in beryl are associated with changes of the electronic state of the iron ion. If the Fe^{2+} ion in the channel is transformed into a Fe^{3+} ion, its size becomes so small that it could enter the Li site next to a missing Be. This possibility should be considered in studies of iron impurities in beryl.

Na^+ in the ring: experimental results for H_2O

The position of the water molecule in the cavity next to the H° atom can be determined by EPR. The intensity of the H satellite line in Fig. 2 is 18% of that of the Al satellite line. After compensation for the partial saturation of the Al line, the correct value is found to be 12%. Since $R_{Al} = 0.152\%$, we obtain $R_H = 0.0182 \pm 0.0030\%$ in a field of 1.275 tesla.

The intensity of the H satellite line was also measured in a lower magnetic field. The spectrum of the satellite lines in a field of 0.350 tesla is shown in Fig. 5. The resolution of the satellite lines is reduced in the lower field, but the H satellite lines are still well resolved. Additional lines are also appearing in the spectrum. These are caused by the simultaneous flipping of two nuclear spins together with the electron spin. The Li satellite line is overlapped by the Al + Be line. Since the Al satellite line is not resolved, the factor *R* for the H satellite line can only be obtained by comparison with the intensity of the main line. In spite of the improved signal-to-noise of the H satellite line at the lower field, the result is less accurate than that obtained at the high field, as can be seen in Table 1. This is due to the additional error sources in the direct comparison. From the result published by Andersson (1974) one obtains $R_H = 0.245\%$ for 0.350 tesla. The intensity of the satellite line is inversely proportional to the square of the magnetic field strength, so this result corresponds to $R_H = 0.0185 \pm 0.0050\%$ at 1.275 tesla. In spite of the large possible errors, the results of the two different measurements are very close to each other. A very weak signal was observed in the low field at a distance of double the proton splitting from the main line, with an amplitude of about 0.3% of that of the H satellite. This shows that two protons can flip simultaneously with the electron, which makes it very likely that the H satellites arise from a water molecule.

When the hydrogen atom with the unpaired electron is located in Cavity B, the closest water molecule is located in Cavity C or Cavity D. It is assumed that this is Type II water with the oxygen located at the center of the cavity and the two hydrogens directed towards Cavity B. The unit cell dimension *c* is 9.246 Å in the tetrahedral beryl example (Brown and Mills 1986). The distance of the hydrogens to the center of Cavity B is

then 4.107 Å. In this configuration, the average value of S_H for 54.74° is 0.415 for two protons. The angle between the direction to the hydrogens and the c-axis is 10.6°, which is in good agreement with the maximum of dipole broadening observed at $\phi = 10°$ by Andersson (1974). The calculated value of S_H is very small for $\phi = 0°$ and 90° and the H satellite almost disappears in the spectra taken at these angles. With $S_H = 0.415$ and $r = 4.107$ Å, $R_H = 0.0206\%$ in a field of 1.275 tesla. Another possibility is that the center of gravity and not the oxygen of the water molecule is located at the center of the cavity. With $S_H = 0.416$ and $r = 4.171$ Å we then get $R_H = 0.0189\%$, which is close to the measured values.

One can also calculate the distance to the protons from the measured value $R_H = 0.0182 \pm 0.0030\%$ at 1.275 tesla. With $S_H = 0.415$ it is 4.19 ± 0.10 Å. The error limits do not exclude that the water molecule can be located with its oxygen atom at 2a, but the results fit better with the distance of 4.171 Å when it is located with the center of gravity at 2a. In the normal beryl, the distance is 4.143 Å when the water molecule is located with its center of gravity at 2a. The distance in Maxixe-type beryl can only be calculated when its unit cell dimensions are known, but the measured distance of 4.19 Å fits best with that in the tetrahedral beryl.

Na^+ in the ring: discussion

Other configurations of water molecules in the channel should also be considered. If there is a Type I water molecule in Cavity C, the distances from the unpaired electron to its protons are 3.910 and 5.412 Å. The H satellite intensity from the nearest proton with $S = 0.213$ is then 0.0142% at 1.275 tesla. With the contribution from the second proton, the total intensity is 0.0162%, which is within the error limits of the measured value. The intensity resulting from two Type I water molecules located in Cavities C and D is twice as high, so that case can be excluded. However, if the two water molecules are located as in Fig. 4, the four protons at a distance of 4.721 Å give an intensity of 0.0176%. This value is very close to the measured result, but this configuration is very unlikely and, as we shall see in the next section, the EPR center is most likely created when there is only one water molecule next to it.

Type II water is the most common kind of water molecules in high-impurity beryl crystals, like the Maxixe-type beryl. Even if the other types of orientation of the water molecule cannot be excluded due to the possible error in the EPR results, it is very likely that the H satellite lines arise from one Type II water molecule, either in Cavity C or in Cavity D. Its protons are directed towards the hydrogen atom in Cavity B and its center of gravity is located at 2a.

There is no Na satellite line observed in the EPR spectrum. The Type II water molecule in Cavity C should be stabilized by a Na^+ ion. This ion cannot be in Ring N, since this would disturb the H° atom. It is therefore located in Ring O, which is in agreement with the assumption that the water hydrogens point towards Cavity B. At this position, $S_{Na} = 2/9$ and $r_{Na} = 6.935$ Å. This gives $R_{Na} = 0.0024\%$ in a field of 1.275 tesla. However, the Na satellite cannot be observed, because it is overlapped by the Al satellite due to the very similar magnetic moments. On the other hand, its contribution to the intensity is so small that it does not significantly change the results. It would correct the measured value for R_H from 0.0182 to 0.0184% in a field of 1.275 tesla.

OH^- in the channel

The discussions in this section and in the following section are hypothetical, because the existence of OH^- ions in the beryl channel has not been definitely proven. Some bands in the infrared spectrum of beryl crystals have been related to OH^- ions in the channel, e.g. by Aurisicchio et al. (1994), but there has been no such strong evidence for their existence as for the OH^- ions in the lattice, observed by Manier-Glavinaz et al. (1989). The assumption that OH^- ions diffuse through the beryl channel leads to different conclusions, which will be compared with observations made in the crystals. In the following section it will be shown how the presence of CO_3^{2-} and NO_3^- ions in beryl can be explained by the diffusion of OH^- ions. Many of the processes described have very small probability, but during the millions of years for which the crystal has existed, they can have occurred numerous times.

A simplified model of tetrahedral beryl contains 4 Al, 5 Be, 1 Li, 1 Na and 2 H_2O in the unit cell with its two cavities. Natural crystals have been found with impurity contents approaching these values. In order to accommodate these impurities, Na has to be located in every second ring and a water molecule in every cavity. One of the two water molecules surrounding each Na is located in a cavity with Li next to an empty Be site. The other water molecule is in a cavity without Li. Water molecules can spontaneously dissociate into H^+ and OH^-, which usually again recombine to H_2O. When the water molecule in the cavity without Li dissociates, the proton can be trapped at a Li site before the recombination to compensate for the missing Be charge. The charge of the Na^+ ion will now be used to neutralize the charge of the OH^- ion remaining the channel.

Referring to Fig. 1 and considering Case (2), where one Na^+ ion is located together with one water molecule in Cavity B, a similar situation as above will be described for a crystal with fewer impurities, where Cavity D is empty. The water molecule in Cavity B dissociates and the proton is trapped at a Li site next to the missing Be. The Na^+ ion is now no longer needed for charge compensation and moves into the empty Cavity D. Its charge is neutralized by the OH^- ion, which is also assumed to diffuse into Cavity D. If there is a water molecule in Cavity E, it and the OH^- ion will stabilize

the Na^+ ion in Ring P. Such a H_2O–Na^+–OH^- configuration has been postulated by Aurisicchio et al. (1994) to explain the OH absorption observed in infrared spectra at 3658 cm^{-1}. This is the most credible reference to the trapping of an OH^- ion in the beryl channel, but since band C in the infrared spectrum may consist of several overlapping absorptions, the interpretation is difficult.

Cavity B now contains only the trapped H^+ and Rings N and M are empty. This gives the perfect surrounding for H° in Cavity B, where it is observed as an almost free atom (Andersson 1974) after the proton has captured an electron released by irradiation. A Type II water molecule in Cavity C gives rise to the proton satellites observed in the EPR spectrum. If the oxygen of the OH^- ion is located at 2a in Cavity D with the proton on the *c*-axis, its contribution to the H satellite intensity at 0.350 tesla is 0.29%, which is larger than that from the water molecule. Since no such additional intensity is observed, there is no OH^- trapped in Cavity D. One explanation could be that Cavity E is also empty and the OH^- ion diffuses beyond Ring P together with the Na^+ ion to form the H_2O–Na^+–OH^- configuration at a more distant location. Still, there must statistically be some water molecules in Cavity E. Since no fraction of the expected H satellite contribution is observed, this may be an indication that the OH^- ion cannot be easily trapped together with H_2O. In that case, it is assumed that the OH^- ion continues to diffuse through the beryl channel until it recombines with another proton or comes across a CO_2 molecule, which will be discussed in the next section.

A simplified model of octahedral beryl contains 3 Al, 1 Mg, 6 Be, 1 Na and 2 H_2O in the unit cell. One of the two water molecules surrounding the Na may dissociate into one proton and one OH neutralizing the Na. This proton cannot be trapped at a Li site, since all Be sites are filled. Instead, it can be trapped by the other water molecule to form a hydronium ion H_3O^+. This H_3O^+–Na^+–OH^- configuration can offer an alternative explanation to the negative peaks observed in neutron diffraction experiments by Artioli et al. (1995). They observe a large peak intensity on the crystal *c*-axis at 0.96 Å from the center of the cavity, which corresponds to the OH distance in a water molecule. The other peaks are distributed in rings with a radius of 0.9 Å above and below the center of the cavity. These signals were interpreted to arise from a water molecule at 2a with the H–H vector at an angle of 38° with the *c*-axis. Instead, the peak on the *c*-axis may come from the OH^- proton and the other peaks from the hydrogens of the hydronium ion. This ion must, however, be considerably flattened to fit the proton positions observed in the neutron diffraction diagram. This flattening would improve the short-range charge compensation, since the positive charge comes closer to the Al sites. The crystal investigated by Artioli et al. (1995) contains almost the number of impurities mentioned above (Fe^{3+} = Al, Fe^{2+} = Mg, the inner ring in the diagram corresponds to the distance of the few Type I water protons), and it would be interesting to study the infrared spectrum of this Irish blue beryl to find any evidence of a trapped OH^- ion.

If the H_3O^+ ion is trapped in the beryl cavity and the crystal is irradiated, a released electron could be captured by the H_3O^+ ion to form a H_3O radical. This would then be a good opportunity to detect the elusive hydronium radical. An EPR signal with axial symmetry around the *c*-axis and with the 1:3:3:1 splitting expected for this radical is observed in Maxixe-type beryl. However, Maxixe-type beryl is not an octahedral beryl and the splitting is much smaller than that expected from theoretical calculations and corresponds to the splitting measured for a CH_3 radical. Such a radical can be created by irradiation of CH_4, which is also found in the beryl channel and is an additional source of protons.

CO_2, NO_2 and the natural colour of Maxixe beryl

It is known from infrared absorption measurements (Wood and Nassau 1967) that CO_2 molecules can exist as impurities in beryl. CO_2^- radicals created by electron capture have been observed in Maxixe-type beryl by EPR as described above. Some suggestions will now be given how the CO_3^- and NO_3 radicals observed by Andersson (1979) could have been formed from CO_2 and NO_2 molecules and the diffusing OH^- ions. The CO_3^- and NO_3 radicals give the blue colour to Maxixe-type and Maxixe beryl, respectively. The CO_3^{2-} ion will be identified as the plug in the beryl channel.

In order to explain the intensity of the EPR signals from Maxixe-type beryl, the unirradiated crystal must have contained at least one CO_3^{2-} ion per 20,000 cavities. The simplest explanation is that these CO_3^{2-} ions were trapped during the formation of the beryl crystal. Another explanation is that the CO_3^{2-} ions were created by CO_2 molecules which have trapped OH^- ions diffusing through the channel. The resulting HCO_3^- ion is likely to split off the proton, which will be trapped at a nearby Li site to release a Na^+ ion from Be^{2+} charge compensation. Together with the Na^+ connected with the OH^-, it will instead compensate for the charge of the CO_3^{2-} ion. The CO_3^{2-} ion forms a very effective plug in the beryl channel, especially if the charge-compensating Na^+ ions are located in the rings surrounding its cavity. This explains the fact that water is released from beryl only at very high temperatures. With one CO_3^{2-} per 20,000 cavities, there is one such plug every 10 μm along the beryl channel.

When the beryl crystal is irradiated, one electron is removed from the CO_3^{2-} ion and is caught by a proton at a Li site to form the H° atom observed in the EPR experiments. This assumption is supported by the facts that the intensity of the H° signal and the CO_3^- signal in the EPR spectrum is about the same and that they disappear simultaneously when the crystal is heated to 180°C. It was also found that these two signals and the

colour were recreated when the bleached Maxixe-type beryl was irradiated by a UV lamp.

Three strong signals are observed in the EPR spectrum from Maxixe beryl (Andersson 1979), one from NO_2, one from NO_3 and one from H°. The NO_2 in Maxixe beryl corresponds to CO_2 in other beryls and the OH^- ions diffusing through the channel may get trapped by NO_2 in Maxixe beryl to form HNO_3^-. The proton and one electron are split off and combine to H° in an empty cavity. The charge of the remaining NO_3^- ion is compensated by the Na^+ ion which diffused together with the OH^- ion. If it is more likely that natural radiation ejects an electron from NO_3^- than from H°, there will be an accumulation of NO_3 as a result of radiation damage during the ages. The final amount was then sufficient for the Maxixe beryl to show a blue colour when it was taken out of the mine (Wild 1933). The ejected electron will combine with the proton trapped in Cavity B to form additional H°. This is one possible explanation of the observed EPR signals. Prolonged exposure of Maxixe beryl to sunlight released electrons from H° and the blue colour vanished when these electrons were captured by NO_3 to form NO_3^-. If the suggested process with the combination of proton and electron to H° is correct, it should also be possible to observe the H° signal in bleached Maxixe beryl, when the NO_3 signal has disappeared.

Beryl structure

The beryl crystal can be divided into three different regions: the stacks of silicate rings, the channel at the center of the rings and the space between the stacks. Most of the impurities in beryl are located within the channel and have little influence on the structure. Al and Be ions are located in the space between the stacks and are keeping the stacks together. Several different impurity ions can substitute for Al, while a missing Be is seldom replaced. Li impurity ions which compensate for the charge of missing Be are located within the stack. Si is also located within the stack and is seldom replaced by an impurity. A model of the beryl structure will now be presented and it will be used to explain some of the distortions of the beryl structure due to impurities. The positions of the oxygens in the beryl structure are calculated from the model and are compared with the positions obtained from room temperature X-ray investigations. The comparisons show that Li is not located at the Be site and that the presence of Na in the oxygen rings reduces the radius of these rings.

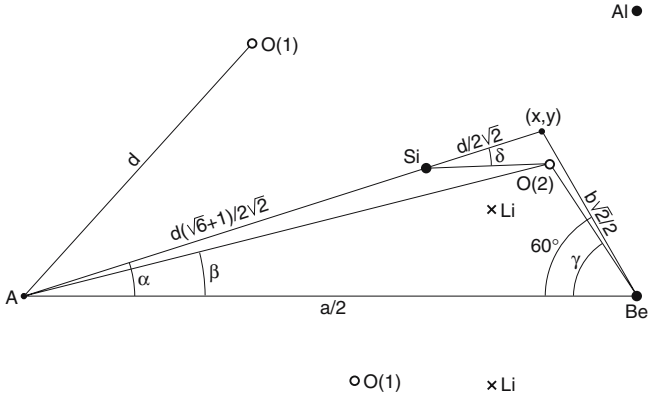

Fig. 6 The projection of some atomic positions in beryl on a plane perpendicular to the crystal *c*-axis with distances obtained from the crystal structure model. The displacement of the O(2) oxygen projection from the position (x,y) of the model is greatly exaggerated in order to better illustrate the different angles

Structure model

In a simplified model of the beryl structure, the silicate rings in the stacks are considered to be formed of regular Si tetrahedra. In the regular Si tetrahedron, the edge between the O(2) oxygens is parallel to the *c*-axis direction and the edge between the O(1) oxygens lies in the perpendicular plane. The length of these edges is *d*. The O(1) edges of different Si tetrahedra are connected to form a hexagon around the point 2b on the hexagonal symmetry axis. The distance from 2b to an O(1) oxygen is then also *d*. The distance from 2b to Si in the regular tetrahedron is $d(\sqrt{6}+1)/2\sqrt{2}$. This is illustrated in Fig. 6, which shows the projections of the atoms in the beryl structure on the plane perpendicular to the *c*-axis and where the projection of 2b is denoted A. The projection of the O(2) oxygens in the regular Si tetrahedron on this plane is denoted (x,y) and the distance from A to this point is $d(\sqrt{6}+2)/2\sqrt{2}$.

The Be atom is first considered to be at the center of a cube with oxygens in every second corner. Lines connecting these oxygens are diagonals of the cube sides and form a regular tetrahedron. The unit cell contains an additional tetrahedron formed from a cube where the other corner positions are occupied by oxygens. In the projection on the plane, the O(2) oxygens of the cube corners form a square with Be at its center and with a side length *b*. The sides of the Be squares can form a regular hexagon with side length *b* around the projection of the Al atom. In this geometry, $b = a/(3+\sqrt{3})$ or $0.2113a$, where *a* is the length of the unit cell along the *a*-axis. The distance measured in normal beryl between the oxygen planes of the Be tetrahedra in the *c*-axis direction is $0.2090a$ (Morosin 1972), which is close to the calculated length *b* of the cube edge.

The crystal *a*-axis is directed from A towards the projection of Be in Fig. 6. The angle α between the *a*-axis and the vector from A to the point (x,y) is 15° in the described geometry. The projection of the O(2) oxygens in the adjacent silicate ring falls at $(x,-y)$. The rings are then rotated 30° with respect to each other. This symmetry gives the closest packing of the silicate rings, with minimum distance between the rings in the *c*-axis direction.

In the perpendicular direction, the distance between neighbouring stacks is determined by the form of the Be

tetrahedra. The tetrahedra must be compressed in the *a*-axis direction to obtain a closer packing of the stacks. It is assumed that the tetrahedron is compressed so much that the angle between the *a*-axis and the line between the projections of Be and the O(2) oxygens changes from 45° in the square to 60°. The projections of all O(2) oxygens in the unit cell will then be located on lines between Be projections. It is also assumed that the distance between the oxygen planes remains as b and that the Be–O distance does not change. The distance between Be and (x,y) in the projection is then still $b\sqrt{2}/2$. The Al hexagon is also distorted as a result of the compression.

In the model with the distorted Be tetrahedron the distance between the oxygens closest to each other in the *a*-axis direction is $b\sqrt{3}/\sqrt{2}$ or $1.2247b$. With $b = 0.2113a$ this becomes $0.2588a$ and with $a = 9.2088$ Å from Morosin (1972) the distance becomes 2.383 Å. This is a very short O–O distance, but in agreement with the 2.355 Å measured in the normal beryl example. The other distances between the oxygens in the Be tetrahedron are $b\sqrt{2}$ or 2.752 Å and $b\sqrt{5}/\sqrt{2}$ or 3.077 Å. The measured values 2.688 and 3.012 Å are smaller than those from the model, so the correct projection of the O(2) oxygens has been put closer to the *a*-axis in Fig. 6 than the point (x,y) of the model.

The model, in which the Si tetrahedron is perfectly regular, can predict the position of Si with great accuracy. The coordinates of the projection of the O(2) oxygens in the model are $x = a/2 - b\sqrt{2}/4$ and $y = b\sqrt{6}/4$, which gives $\alpha = 16.93°$. This angle, which is defined in Fig. 6, is obtained from $tg\alpha = y/x = \sqrt{3}/\left(\sqrt{2}\left(3+\sqrt{3}\right)-1\right)$. In the model, the distance from point A to the O(2) projection is the square root of $x^2 + y^2$. Since this distance is also $d\left(\sqrt{6}+2\right)/2\sqrt{2}$, we find that $d = 0.2826a$. The distance from A to Si is $d\left(\sqrt{6}+1\right)/2\sqrt{2}$, which then is $0.3447a$. The experimental values obtained for Si from the parameters of Morosin (1972) are 16.93° and $0.3445a$. The distance from Si to the projection of the O(2) oxygens is $d/2\sqrt{2}$ or $0.0999a$, which is equal to the measured $0.0999a$. The unit cell parameter $c = 2(b + d) = 0.9878a$ in the model, which is 1% smaller than the $0.9979a$ measured in the normal beryl.

The angles to the correct projection of the O(2) oxygens are defined in Fig. 6 and are measured to be $\beta = 16.48°$ and $\gamma = 59.61°$. The distortion of the Si tetrahedron is described by the angle δ, which is 2.02°. The bisector of the O(1)–Si–O(1) angle deviates only 0.02° from its direction in the undistorted model, which shows that the positions of the O(1) oxygens, which are locked in the ring, are minimally influenced by the displacement of the O(2) oxygens.

Why is the Si tetrahedron distorted so that the projection of the O(2) oxygens does not fall at the point (x,y)? When the Be tetrahedron is distorted by the closer packing of the stacks, the separation of its oxygen projections in the direction normal to the *a*-axis is increased. This corresponds to a rotation of the rigid silicate rings, so that neighbouring rings are orientated more than 30° from each other. In the model, this rotation is 34° (two times 16.93°), while in the normal beryl the angle between the directions to the oxygen projections is 33°, as illustrated in Fig. 4. The rotation away from 30° moves the silicate rings further from each other in the *c*-axis direction. If the O(2) oxygens are rotated less than the O(1) oxygens, the distance between the rings in the *c*-axis direction is reduced. The distortion of the Si tetrahedron therefore allows a closer packing of the silicate rings in the stack. This also explains why the distance of $0.2090a$ measured between the oxygen planes of the beryl tetrahedra in the *c*-axis direction is smaller than the $0.2113a$ calculated from the model.

The Al–O distance is 1.890 Å and the Be–O distance is 1.685 Å in the beryl model when the lattice parameter $a = 9.2088$ Å. The measured values in the normal beryl are 1.904 and 1.653 Å, which are in the range expected for Al octahedra and Be tetrahedra. The Al–O distance of 1.890 Å is very short, which may also be a reason why the O(2) oxygens are moved closer to the Be site. The short Al–O distance prevents a closer packing of the stacks.

Structure distortion by impurities

The impurity ions substituting for Al are usually larger than the Al ion. Since the Al octahedron is already very small for Al, such substitution cannot occur without lattice distortion. The Al sites are located between the stacks and the introduction of larger ions at these sites increases the distance between the stacks. This increases the unit cell parameter *a* in octahedral beryl, which has been observed e.g. by Bakakin et al. (1970) and Aurisicchio et al. (1988), who characterize octahedral beryl by a low c/a ratio. The distortion can be measured more directly by the size of the Al hexagon in the projection on the plane perpendicular to the crystal *c*-axis. The circumference of the Al hexagon is 10.147 Å in octahedral beryl, while it is 9.825 Å in normal beryl and 9.828 Å in tetrahedral beryl. Here, as well as below, the parameters for tetrahedral beryl are obtained from Brown and Mills (1986), for octahedral beryl from Artioli et al. (1995), and for normal beryl from Morosin (1972). Additional data are obtained from Sherriff et al. (1991), and it is found that the circumference is 9.830 Å in their low-impurity beryl and around 9.79 Å in their tetrahedral beryls.

The Be ions are also located between the stacks. If they are replaced by the much larger Li ions, the distance between the stacks is expected to increase. However, the hexagon circumference in tetrahedral beryl, which contains Li impurities, is not larger than the circumference in normal beryl. This is one piece of evidence that the Li ions are not located at the Be sites.

The projection of the Li site on the plane perpendicular to the *c*-axis is indicated with a cross in Fig. 6. When Li ions occupy Li sites, the angles α and β are expected to increase. In the tetrahedral beryl, the angle α

is increased by 0.41° from 16.93° to 17.34° and the angle β is increased by 0.17° from 16.48° to 16.65°. If the Li ions were located at the Be sites, one would expect the angle β to increase more than the angle α. One would also expect that the angle δ should be smaller than 2.02° if the larger Li ion is located at the Be site. Instead, it is measured to be 3.11° in tetrahedral beryl. This increase can be expected if many of the Be sites are empty. Therefore, already the X-ray results make it clear that the Li ion does not occupy the Be site.

The presence of Li impurities between the oxygen layers of the Be tetrahedra increases their distance in the *c*-axis direction. The distance between the layers is 1.951 Å in the tetrahedral beryl example, while it is 1.924 Å in the normal and 1.930 Å in the octahedral beryl. The calculated coordinates for the Li site are (0.426, 0.342, 0.164) in the octahedral beryl and (0.423, 0.344, 0.167) in the normal beryl. In the tetrahedral beryl, where this site is occupied, the coordinates are (0.423, 0.343, 0.167). This is almost the same as in the normal beryl and shows that the lattice expansion in tetrahedral beryl originates from this point.

The very short O–O distance of 2.355 Å in the Be tetrahedron, measured in the normal beryl, may cause some stress. The distance between these two oxygens is increased to 2.393 Å in the tetrahedral beryl and to 2.395 Å in the octahedral beryl. The increase of this distance in the presence of impurities releases the stress and may be a reason why impurities are so often found in natural beryl.

A different distortion of the Si tetrahedron, in addition to that discussed above, is observed in the presence of impurity ions in the channel rings. It was shown that the O(1) oxygens are practically undisturbed by the displacement of the O(2) oxygens in normal beryl. However, the O(1)–Si–O(1) angle changes from 108.24° in the normal beryl to 105.58° in the tetrahedral beryl and 105.16° in the octahedral beryl. The corresponding radii of the oxygen rings are reduced from 2.584 Å in normal beryl to 2.560 Å in the tetrahedral beryl and to 2.555 Å in the octahedral beryl. This distortion is assumed to be caused by a Na^+ ion at site 2b, which attracts the O(1) oxygens to form a smaller ring. A supporting argument for this is that the same contraction is observed in both tetrahedral and octahedral beryl and only at high impurity concentrations, when type II water molecules stabilize Na^+ in the 2b position. An additional example is taken from Sherriff et al. (1991), where the O(1)–Si–O(1) angle is 107.9° in the low impurity beryl and between 104.9° and 106.0° when the Na concentration is ten times higher.

References

Andersson LO (1974) EPR of hydrogen atoms in beryl crystals. In: Proceedings of 18th Congress Ampere, pp 129–130

Andersson LO (1976) Selective line cancellation in overlapping EPR spectra using 90° out-of-phase detection. Applications to Maxixe type beryl. In: Proceedings of 19th Congress Ampere, p 535

Andersson LO (1979) The difference between Maxixe beryl and Maxixe-type beryl: an electron paramagnetic resonance investigation. J Gemm 16:313–317

Artioli G, Rinaldi R, Wilson CC, Zanazzi PF (1995) Single-crystal pulsed neutron diffraction of a highly hydrous beryl. Acta Crystallogr B51:733–737

Aurisicchio C, Fioravanti G, Grubessi O, Zanazzi PF (1988) Reappraisal of the crystal chemistry of beryl. Am Mineral 73:826–837

Aurisicchio C, Grubessi O, Zecchini P (1994) Infrared spectroscopy and crystal chemistry of the beryl group. Can Mineral 32:55–68

Bakakin VV, Rylov GM, Belov NV (1969) Crystal structure of lithium-bearing beryl. Dokl Acad Nauk SSSR 188:659–662

Bakakin VV, Rylov GM, Belov NV (1970) X-ray diffraction data for identification of beryl isomorphs. Geokhimiya 11:1302–1311

Bastos FM (1975) Maxixe type beryl. Lapidary J 28:1540–1542

Bragg WL, West J (1926) The structure of beryl $Be_3Al_2Si_6O_{18}$. Proc R Soc London Ser A III:691–714

Brown GE, Mills BA (1986) High-temperature structure and crystal chemistry of hydrous alkali-rich beryl from Harding pegmatite, Taos County, New Mexico. Am Mineral 71:547–556

Gibbs GV, Breck DW, Meagher EP (1968) Structural refinement of hydrous and anhydrous synthetic beryl, $Al_2(Be_3Si_6)O_{18}$ and emerald, $Al_{1.9}Cr_{0.1}(Be_3Si_6)O_{18}$. Lithos 1:275–285

Hawthorne FC, Cerny P (1977) The alkali-metal positions in Cs–Li beryl. Can Mineral 15:414–421

Manier-Glavinaz V, Couty R, Lagache M (1989) The removals of alkalis from beryl: structural adjustments. Can Mineral 27:663–671

Morosin B (1972) Structure and thermal expansion of beryl. Acta Crystallogr B28:1899–1903

Nassau K, Prescott BE, Wood DL (1976) The deep blue Maxixe-type color center in beryl. Am Mineral 61:100–107

Schmetzer K (1989) Types of water in natural and synthetic emerald. N Jb Miner Mh 1:15–26

Sherriff LS, Grundy HD, Hartmann JS, Hawthorne FC, Cerny P (1991) The incorporation of alkalis in beryl: multi-nuclear MAS NMR and crystal-structure studies. Can Mineral 29:271–285

Trammel GT, Zeldes H, Livingston R (1958) Effect of environmental nuclei in electron spin resonance spectroscopy. Phys Rev 110:630–634

Wild GO (1933) Mitteilung über ein enscheinend neues Berylliumsilikat. Zentralbl Mineral Geol Paläont 1933A:38–39

Wood DL, Nassau K (1967) Infrared spectra of foreign molecules in beryl. J Chem Phys 47:2220–2228